AIMS Environmental Science, 4(2): 289-309.
DOI: 10.3934/environsci.2017.2.289
Received: 10 December 2016
Accepted: 5 March 2017
Published:17 March 2017

http://www.aimspress.com/journal/environmental

Research article

A CFD study for evaluating the effects of natural ventilation on indoor comfort conditions

Miguel Mora-Pérez [1], Ignacio Guillen-Guillamón [2] and Petra Amparo López-Jiménez [1,*]

[1] Department of Hydraulic and Environmental Engineering, Universitat Politècnica de València, Camino de Vera s/n 46022 Valencia, Spain
[2] Department of Physics, Universitat Politècnica de València, Camino de Vera s/n 46022 Valencia, Spain

*** Correspondence:** Email: palopez@upv.es; Tel: +34-96-387-7000.

Abstract: There is an increasing interest in improving energy efficiency in buildings due to the increased awareness about environmental impact and energy cost. Natural ventilation is an environmentally friendly technique which has become more attractive way for reducing energy use while it also provides acceptable comfort conditions. The research shows a case study building in which the natural ventilation effect due to wind-driven forces on indoor comfort conditions is evaluated. Moreover, the architectural solutions selected during the building design phase to improve the natural ventilation behaviour are successfully validated in a full-scale building. The indoor comfort conditions are evaluated through contrasted performance indicators: draught risk (*DR*), predicted percentage of dissatisfied people (*PPD*) and predicted mean vote (*PMV*) indexes. The results show that air movement due to natural ventilation allows increasing indoor air temperature maintaining the initial comfort conditions. Therefore, the mechanical air conditioning use can be postponed until the indoor air temperature is high and would, consequently, reduce the total building energy consumption. Thereby, a proper natural ventilation focus during the initial design stage could improve the building energy efficiency without compromising the indoor comfort conditions.

Keywords: natural ventilation; energy efficiency; comfort conditions; computational fluid dynamics

Nomenclature:

Magnitude	Unit	Description	Magnitude	Unit	Description
W	W	Active work	v_{RMS}	m/s	Average wind or air speed
Fcl		Clothing area factor	Tcl	ºC	Clothing surface temperature
hc	$W/m^2 \cdot K$	Convective heat transfer coefficient	μ	m^2/s	Eddy viscosity
ρ	kg/m^3	Fluid density	g	N	Gravitational force
z	m	Height	S_m	kg	Mass
$Ø_{i,obs}$	m/s	Mean measured value for i point	Tr	ºC	Mean radiant temperature
M	W/m^2	Metabolic energy production	N		Number of analysed points
F	N	Outer force	Pa	Pa	Partial water vapour pressure
α		Power law exponent	$Ø_i$	m/s	Predicted value for i point
z_r	m	Reference height	$U(z_r)$	m/s	Reference wind speed at height z_r
h_0	m	Roughness height	p	Pa	Static pressure
$\bar{\tau}$		Stress tensor	H_{max}	m	Tallest building height
Icl	clo	Thermal clothing insulation	L	W/m^2	Thermal load on the body
t	s	Time	Tu	%	Turbulence intensity
k	m^2/s^2	Turbulent kinetic energy	I		Unit tensor
D	m	Urban represented area width	Ta	ºC	Wind or air temperature
v	m/s	Wind or air velocity	U(z)	m/s	Wind speed at height z

1. Introduction

The increasing global concern about the environment has increased the demand for energy efficient buildings during the last few decades. In this sense, the use of passive mechanisms is being promoted to take advantage of natural energy resources. Complementally, a certification procedure has been developed in order to regulate a given prominence to sustainable designs [1]. Innovative design methods and solutions are becoming more popular to achieve environmentally friendly buildings [2,3]. In this framework, natural ventilation (NV) has become an increasingly sustainable method for reducing the buildings energy operational cost. Natural ventilation is a passive mechanism that takes advantage of wind energy resources to achieve acceptable comfort conditions in buildings. Moreover, lower operative energy consumption as well as improved indoor environmental quality are included in the potential benefits of NV [4]. NV is based on pressure differences to exchange indoor air with outdoor air without any mechanical system. The system relies on pressure differences caused either by wind or by buoyancy forces.

The implementation of natural ventilation systems presents certain challenges, especially in the systems in which the wind driven effect ought to be maximized. In this sense, the main challenge is to minimize the draught risk and ensure comfort conditions. Designers have to ensure that the initial design solutions made during the design phase will work once the buildings have been built. NV has been traditionally investigated for more than 50 years using experimental techniques [5]. However, as experimental measurements cannot be done before building construction; software and numerical methods are necessary to simulate outdoor and indoor environments in order to predict NV behaviour [6,7] and ensure acceptable comfort conditions [8]. Consequently, traditional

design techniques should be combined with innovative methodologies based on numerical methods.

Mathematical methods based on computational fluid dynamics (CFD) have become one of the most used techniques to determine NV flows recently [9]. CFD allows testing several building design solutions avoiding the full scale construction considering different environmental conditions, which results in an efficient design method. Despite CFD allows simulating environmental conditions, results must be validated with experimental measurements. Experimental results are a must to ensure the reliability of a CFD model; otherwise, wrong conclusions could be obtained regarding the building energy performance. Moreover, the importance of CFD validation before the building construction is that once the building is built, no other architecture solutions can be assessed. Accordingly, results obtained from simulations must be reliable enough to ensure a proper initial building design.

Simulation models have mainly been used in existent buildings to assess energy efficiency solutions [2,10-12]. Moreover, there are less preliminary NV behaviour studies in residential buildings. However, the NV assessment is a well-established practice for important buildings such as hospitals and high-rise buildings [13-18]. The present research is focused on the indoor comfort conditions evaluation in a case study building that had been designed following a NV design strategy [13,19]. The strategy is based on considering the effect of the local wind, the neighbouring buildings and the building orientation and openings design. The naturally ventilated building is designed taking into account the conditions for acceptable indoor environments of the most relevant standards [20-22]. Nevertheless, it may happen that the predicted NV strategies do not fulfil the initial design criteria [10]. Therefore, the validation of the effect of the initial architectural alternatives selection should be a must.

In the present case, the architectural alternatives have been selected to take maximum profit of the wind driven forces. The one-floor building configuration, which is detailed in the next section, makes the wind-driven forces the main ventilation drivers instead of the buoyancy effect. Complementarily to the natural ventilation thermal effect analysis, as presented in [23], the present contribution is only focused on the analysis of the wind-driven forces effect on comfort conditions and its potential energy savings.

2. Materials and Methods

The present research is conducted in a full-scale building in which the indoor comfort conditions are assessed through CFD techniques. The full-scale building is mainly used for the validation of the CFD simulations.

2.1. Full-scale building description

The case study building is a one-floor building (13.77 m × 5 m), 4 m high. Figure 1 shows the case study building.

Figure 2 shows the internal layout of the case study building and each façade orientation. The figure also represents the fluid region used in the indoor computational model. The indoor has two rooms connected by a short corridor. The main room (A) is connected to the secondary room (B) through the corridor (C). The main room has an outside door south-south-west (SSW) oriented. It is also provided with a 2 × 0.5 m vertical lateral windows east-south-east (ESE) oriented. Figure 3 shows the main room indoor layout. The secondary room has three 1.5 m × 1.2 m windows in the

SSW façade. Each room has narrow windows 0.5 m high placed in the upper part of the north-north-east (NNE) façade. The opening shape and position in the building is the result of the NV design strategy followed by Mora-Pérez et al. [19].

Figure 1. Case study building outside view (south view).

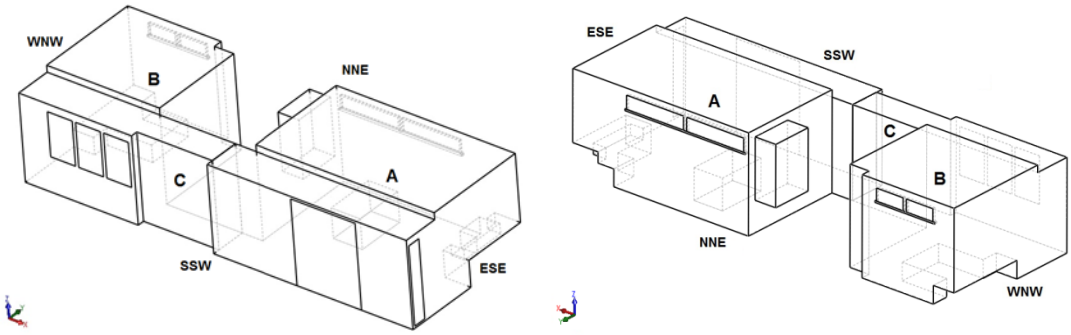

Figure 2. Indoor computational model fluid region.

Figure 3. Case study building indoor view. Main room. (SSW-NNE view).

The building is located close to the Mediterranean Sea in Valencia (Spain). The location and orientation of the building is the result of the NV design strategy followed by Mora-Pérez et al. [13]. The immediate surroundings consist of a 17 m high and 65 m long building located 15.3 m from the ESE building face and two 5.5 and 7 m high buildings placed 5 m from the WNW building face. Figure 4 shows the case study building location and orientation, the near buildings and the surrounding area.

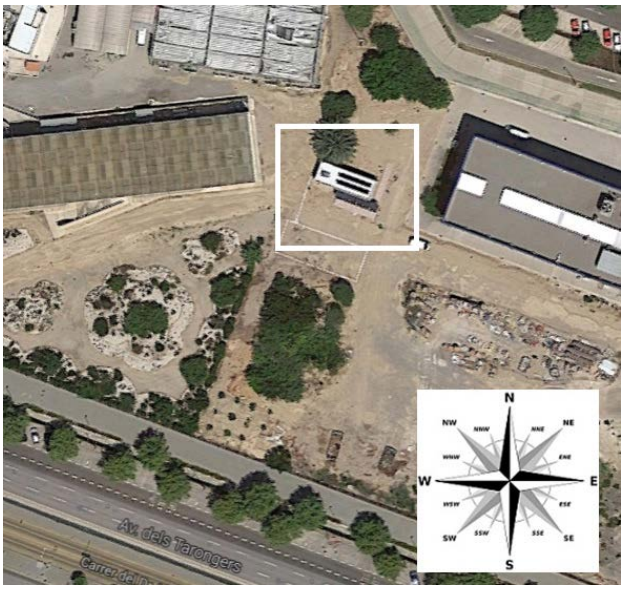

Figure 4. Case study building location and orientation.

2.2. Computational model definition

A commercial CFD software (Star CCM+) is used to predict the indoor air flow behaviour and the comfort indicators in the building. The software simulates the outdoor and the indoor environment in a coupled domain. The outdoor environment is composed only by the relevant surrounding buildings described in the previous section. The indoor environment is represented in more detail because it is the area of interest. In this area, the CFD software calculates and visualizes comfort condition indicators such as draught risk (*DR*), predicted mean vote (*PMV*) and predicted percentage of dissatisfied people (*PPD*) in a 3D volume.

2.2.1. Computational geometry and mesh

In order to reach a balance between detail level and computational time, the geometry that represents the surrounding environment is simplified [24]. The effect of some elements such as trees placed leeward and small elements have already been considered in the terrain roughness height and the wind profile boundary conditions definition that are detailed in the next section. The indoor layout is represented in more detail because the air behaviour in the building is of particular concern. The main static furniture such as the sofa, the bed and the kitchen appliances are modelled in the indoor environment. Figure 5 shows the case study building and the three surrounding buildings previously described.

The outdoor volume is enclosed within 6 walls in which the boundary conditions are defined [13]. The velocity inlet boundary surface is 5 H_{max} away from the case study building in the prevailing wind direction, where H_{max} is the height of the tallest near building (17 m). The outflow is located following the same rule 15 H_{max} in the opposite side and 1.5 D each lateral boundary, where D is the width of the urban area represented. The top boundary is 5 H_{max} away from the tallest building. The domain is divided into small cells using the trimmer volume mesh, which is particularly suitable for modelling aerodynamic flows due to its ability to refine cells in wake regions [24]. The mesh near the indoor area

of interest (≤25 mm) is tighter than the mesh away from the area of interest (≥4 m). In order to verify that the results are independent of cells number, several simulations with different size meshes are performed, i.e., reducing the cell size following the CFD recommendations [25]. There is a limit in which the mesh size reduction does not improve the computational error, whereas the computational time is highly increased. An error of 4.8% appears when comparing CFD results for velocities with different mesh accuracies, while computational time is 54% higher [13]. Therefore, error of 4.8% is assumed as adequate to reach an equilibrium balance within computational time and results accuracy. In this case, the selected model has 766.131 cells [13]. Figure 6 shows the indoor mesh in a horizontal plane.

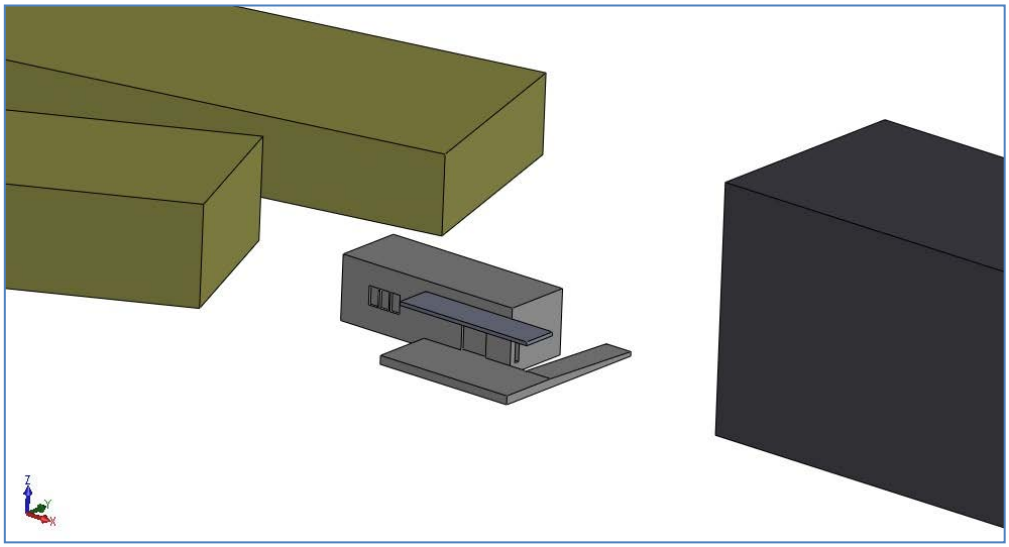

Figure 5. Outdoor CFD model.

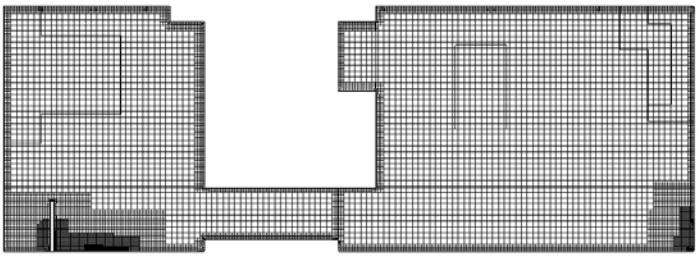

Figure 6. Volume mesh in a horizontal plane. Height = 1.4 m.

2.2.2. Boundary conditions

The outdoor environment is enclosed by 6 boundary conditions set in the limits of the outdoor domain. The wind is simulated by using a velocity inlet profile (east face boundary). Pressure outlet condition simulates the wind sink that is opposite to the velocity inlet boundary (west face boundary). Both lateral and top faces are considered as symmetry planes (south, north and top faces) to enforce

parallel flow. The updated Davenport classification is used to define the roughness height of the ground (h_0 = 0.5 m) [26].

The velocity inlet profile is defined taking into account the wind measurements done from the Universitat Politècnica de Valencia and Valencia meteorological stations [27]. It is quite time-consuming to cover all indoor air scenarios coming from all wind direction so a statistical analysis is done in order to choose the most probable wind direction during summer period: ESE [28]. Furthermore, wind velocities are approximately normally distributed; the wind mean velocity is 3.05 m/s and the standard deviation is 1.47 m/s. Then, the simulations are run with three different wind velocities modulus: the average value 3.05 m/s and the average value plus minus the standard deviation, 1.58 m/s and 4.52 m/s. The air is considered ideal gas.

The power law equation is used to calculate the vertical wind speed profile (1) that is shown in Figure 7.

$$\frac{U(z)}{U(z_r)} = \left(\frac{z}{z_r}\right)^{\alpha} \tag{1}$$

where $U(z)$ is the wind speed at height z (measured in m), $U(z_r)$ is the reference wind speed at z_r = 10 m height and α is the power law exponent [29]. The power law exponent definition is complex because it varies with such parameters as day time, wind speed, temperature, surface roughness and some other mechanical and thermal mixing parameters [29]. In any case these parameters could be mainly classified depending on the surface roughness or on the atmospheric stability [30]. Some authors have proposed empirical methods for calculating it [29]. In this case the selected exponent calculation was proposed by Justus and Mikhail and is function of velocity and height so it depends on the site [31]. The power law exponent is defined by eq (2).

$$\alpha = \frac{0.37 - 0.088 \times \ln(U_r)}{1 - 0.088 \times \ln(z_r/10)} \tag{2}$$

where U is given in m/s and z_r in m.

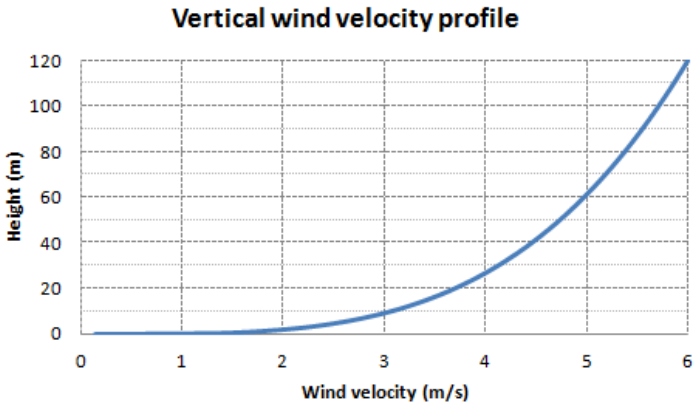

Figure 7. Wind velocity profile.

2.2.3. Solver settings

The mathematical definition of the problem is done through Reynold-averaged Navier-Stokes equations as recommended for NV purposes [32]. The equations are solved in a 3D domain. The modelling technique discretizes the 3D volume in small cells in which mass and momentum conservation equations are solved. K-epsilon and the segregated flow model are used to represent the turbulence [33]. The mass conservation equation is solved by the software (3).

$$\frac{\partial \rho}{\partial t} + \nabla \rho \vec{v} = S_m \tag{3}$$

where ρ stands for the fluid density, t is the time, $\vec{v}$ is the velocity and S_m represents the mass contained in the control volume. Navier-Stokes momentum equation is considered as (4).

$$\frac{\partial (\rho \vec{v})}{\partial t} + \nabla \rho (\vec{v}\vec{v}) = -\nabla p + \nabla \bar{\tau} + \rho \vec{g} + \vec{F} \tag{4}$$

where p stands for the static pressure, $\bar{\tau}$ the stress tensor defined by eq (5) and $\vec{g}$ and $\vec{F}$ represent the gravitational and outer forces respectively. μ is the eddy viscosity and I is the unit tensor.

$$\bar{\tau} = \mu \times \left[\left(\nabla \vec{v} + \nabla \vec{v}^T \right) - \frac{2}{3} \times \nabla \vec{v} I \right] \tag{5}$$

The discretization of the volume is done following the finite volume method [24].

2.3. Indoor comfort indexes analysis strategy

The balance between NV performance and comfort conditions in the occupied spaces is analysed. CFD techniques are utilized to evaluate the indoor comfort conditions initially. *DR* is assessed as the most common cause of local discomfort. The draught caused by air velocity produces an undesired local cooling feeling in the human body [20]. The results of the indoor air velocity are reported in the current paper.

Indoor temperature can be maintained slightly higher than desired to make more energy efficient buildings in summer conditions. The increase in temperature may lead to an air speed increase to achieve similar comfortable feeling, although high air velocity may cause draught discomfort, especially when the air flow may occur on the nude parts of the body. According to Orosa-Garcia research [34], the highest indoor air velocity should be 0.9 m/s in summer conditions. Moreover, *DR* calculation takes into account human heat loss because of air flow. The amount of heat loss depends on the average air velocity, turbulence and temperature. The percentage of people predicted to be dissatisfied due to draught is calculated according to eq (6).

$$DR(\%) = \left(34 - T_a\right) \times \left(v - 0.05\right)^{0.62} \times \left(0.37 \times v \times T_u + 3.14\right) \tag{6}$$

where v stands for the air velocity (m/s), T_a is the air temperature (ºC) and T_u is the turbulence intensity (%). The boundary conditions for this formula are: $20 < T_a$ (ºC) < 26; $0.05 < v$ (m/s) < 0.5 and $0 < T_u$ (%) < 70. Turbulence intensity represents the ratio between average air speed and speed fluctuation (7).

$$T_u = \frac{v_{RMS}}{v} \times 100 \tag{7}$$

in which average air speed and speed fluctuation are computed as following:

$$v_{RMS} = \sqrt{\frac{1}{3} \times \left(v_x'^2 + v_y'^2 + v_z'^2\right)} = \sqrt{\frac{2}{3} \times k} \tag{8}$$

$$v = \sqrt{v_x^2 + v_y^2 + v_z^2} \tag{9}$$

where k is the turbulent kinetic energy (m^2/s^2).

Secondly, *PMV* and *PPD* indoor comfort indexes are evaluated [35]. *PMV* predicts the mean value of thermal sensation votes of a large group of persons on a 7-point scale (+3 too hot, 0 neutral and −3 too cold), eq (10). *PPD* predicts the percentage of a large people group to feel dissatisfied according to thermal conditions, eq (11).

$$PMV = \left(0.303 \times \exp\left(-0.036 \times M\right) + 0.028\right) \times L \tag{10}$$

$$PPD = 100 - 95 \times e^{\left(-0.03353 \times PMV^4 - 0.2179 \times PMV^2\right)} \tag{11}$$

where M is the metabolic energy production; L is the thermal load on the body expressed as eq (12).

$$\begin{aligned} L = {} & M - \frac{3.05}{1000} \times \left(5733 - 6.99 \times \left(M - W\right) - Pa\right) - 0.42 \times \left(M - W - 58.15\right) \\ & - \frac{1.7}{1000} \times \left(5867 - Pa\right) - 0.0014 \times M \times \left(34 - Ta\right) \\ & - 3.96 \times 10^{-8} \times Fcl \times \left(\left(Tcl + 273\right)^4 - \left(Tr + 273\right)^4\right) - Fcl \times hc \times \left(Tcl - Ta\right) \end{aligned} \tag{12}$$

where W is active work, *Tcl* is the clothing surface temperature and *Fcl* is the clothing area factor. The clothing area factor should be according to the thermal clothing insulation (*Icl*) and vice-versa. *Ta* is the ambient temperature in each region of the control volume and *Tr* is the average radiant temperature. *Pa* is the partial pressure of water vapour (considering 50% of relative humidity). *hc* is the convective heat transfer coefficient (internal flow, turbulent flow). The clothing surface temperature is calculated by eq (13)

$$\begin{aligned} Tcl = {} & 35.7 - 0.028 \times \left(M - W\right) \\ & - 0.155 \times Icl \times \begin{pmatrix} 3.96 \times 10^{-8} \times Fcl \times \left(\left(Tcl + 273\right)^4 - \left(Tr + 273\right)^4\right) \\ + Fcl \times h_c \times \left(Tcl - Ta\right) \end{pmatrix} \end{aligned} \tag{13}.$$

Indoor comfort conditions are divided in three categories according to indoor air temperature and *PPD*, *PMV* and *DR* indexes among others [21]. Table 1 shows the indoor comfort conditions evaluation criteria.

Table 1. Thermal environment categories in summer conditions [21].

Category	Indoor air temperature, (ºC)	Predicted percentage of dissatisfied, *PPD*	Predicted mean vote, *PMV*	Percentage of dissatisfied due to draught, *DR*	Maximum mean air velocity, (m/s)
A	24.5 ± 1.0	<6	−0.2 < *PMV* < +0.2	<15	0.18
B	24.5 ± 1.5	<10	−0.5 < *PMV* < +0.5	<20	0.22
C	24.5 ± 2.5	<15	−0.7 < *PMV* < +0.7	<25	0.25

The strategy consists in checking whether similar comfort indexes that are reached with lower air temperatures could be achieved by the only effect of natural ventilation. Therefore, it should be assessed whether equivalent comfort conditions to lower air temperatures are reached with higher air temperatures and higher air velocities due to NV. Consequently the indoor target temperature would be increased maintaining the comfort conditions and improving the energy performance of the building. Three different wind temperatures and three different wind velocities are used to compare *DR*, *PMV* and *PPD* comfort indexes. The indoor air temperature is set at 26, 25.5 and 24.5 ºC in each simulation according to Table 1 category limits [21] and field measurements during the warm season. All the registered temperatures in the measurement interval were included within this interval. Moreover, 26 ºC is used as non-common indoor air temperature because it is higher than the maximum air temperature allowed in the national regulation [36]. The air temperature is fixed in the formula of each comfort condition index. However, the wind velocity boundary is set at three different values for each air temperature in order to cover a wide velocity range and to determine its impact on indoor comfort conditions: 3.05 m/s, 1.58 m/s and 4.52 m/s.

Comfort conditions are analysed in the spaces in which occupants are usually located. The occupied zone is confined by vertical and horizontal planes [37], the vertical planes are placed 0.5 m from the internal walls and 1.0 m from the external windows and doors. The horizontal planes are placed 0.05 m (lower boundary) and 1.8 m (upper boundary) above the floor. Special draught and temperature agreements are done in transit zones, in which it could be difficult to meet the thermal comfort requirements. Figure 8 shows the occupied zone considered in the simulations.

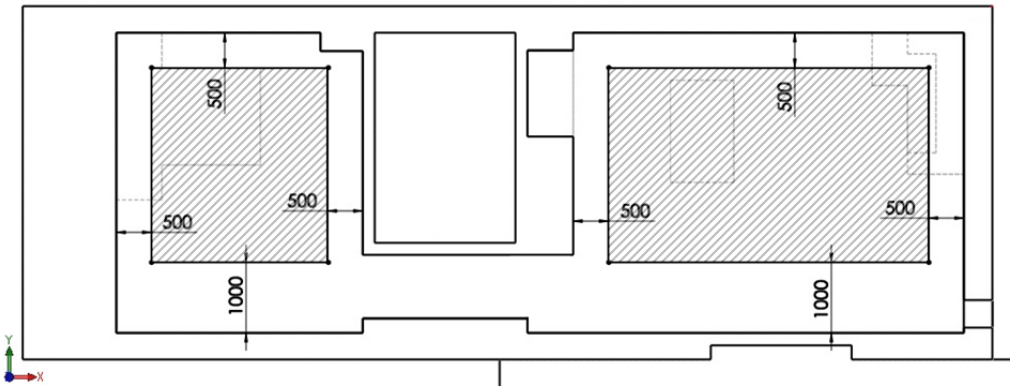

Figure 8. Occupied Zone in the building (units in cm).

2.4. Full-scale measurements

Experimental measurements must be done to validate the CFD simulation reliability. The simulation is validated by comparing the CFD numerical results with experimental measurements. This validation strategy has been successfully used by different authors [7,15,31,38-40]. The indoor velocity sensors are selected to measure the air velocities accurately. The simulated wind speed has a nominal value of 3.05 m/s on a typical windy day during the warm season. Consequently, hot wire air-speed sensors ranged between 0 and 5 m/s are selected. The equipment has an accuracy of ±0.03 + 0.2% m/s (+ 0.2% is the percentage respect the full scale measurement). Figure 9 illustrates the wind measurements considered in a typical ESE direction windy day with an average wind speed near 3 m/s [27]. The period of time in which the indoor measurements could be compared with the CFD calculations are the periods considered quasi-stead-state. That is when the wind fluctuations are not higher than ±20% of the average value during 10 to 30 min intervals. Longer intervals are not feasible because the outdoor conditions are considered steady for less than 30 min [41]. In this case, the period between 11:00 and 12:20 h is considered as a quasi-stead-state period of time.

The indoor measurements are done along six vertical axes in order to determine the air vertical profile in the building. Moreover, the air velocity measurements should be focused on the place in which the human body is more sensible to air flow changes. Thus, the sensor height is chosen according to the position of the nude parts of the human body: 0.5, 1.2 and 1.7 m. These heights are carefully chosen to represent the main nude human body parts location while seated and on foot (face, hands and lower legs). Figure 10 shows the positions where the vertical axes are placed in the building layout.

Position A1, A2 and A3 are used to know the air velocity through the vertical ESE window, the left SSW window and the corridor, respectively. A4 and A5 are placed near commonly used areas in the main room; and finally A6 is located in the secondary room.

Among the multiple opening configurations that could be set in the building, only the most favourable is used to analyse the comfort indexes in the building: Vertical ESE and left SSW windows are opened (90º), NNE upper windows are opened (20º), central and right SSW windows are completely closed. Other opening configurations should be modelled to analyse different ventilation rates and comfort indexes in the future.

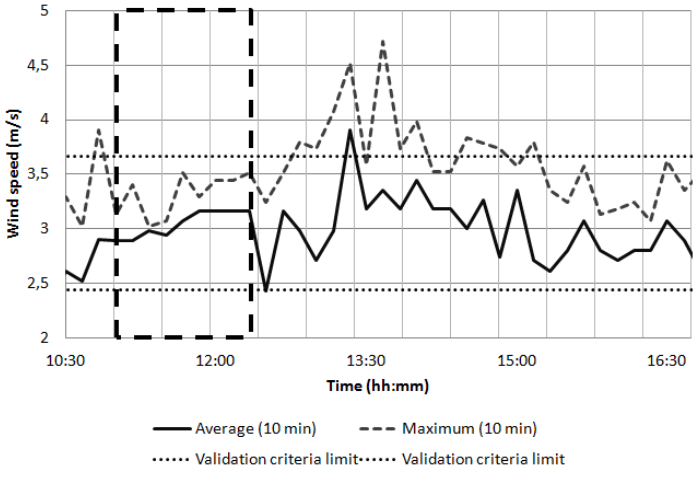

Figure 9. Typical daily wind profile in the warm season [27].

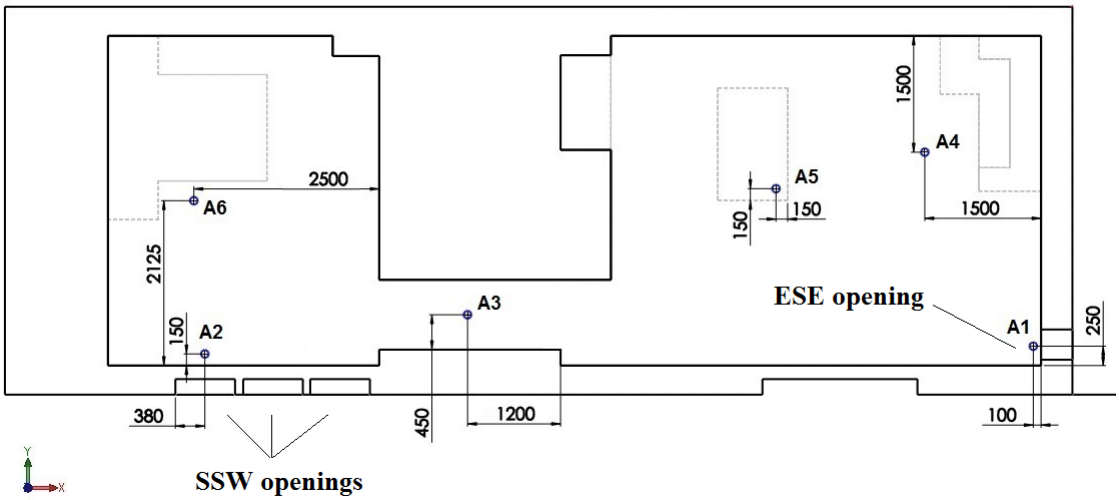

Figure 10. Vertical axes sensors location (units in mm).

3. Results and Discussion

Indoor full-scale measurements are used to determine the real NV behaviour and validate the CFD simulation. Then, the simulation is used to analyse human comfort under different natural ventilation conditions.

3.1. CFD indoor model validation

The validation is carried out comparing full-scale measurements and CFD calculations. The measurement validation criteria is set at 0.04 m/s absolute difference between measured average air speed and simulated air speeds. This velocity value accounts for 9.70% of the measured average air speed, which is smaller than 10% as indicated in [38]. Figure 11 shows the CFD calculations together with the full-scale measurements. The CFD results are represented along the complete building height (vertical lines) and the full-scale measurements are represented at each point by a horizontal line (it shows the measurement range, minimum and maximum values) and the nominal value. The indoor measurements are taken when the average wind speed meets the conditions depicted in section 2.4. Moreover, the indoor measurements are done in some points according to section 2.4. The graphed results show a good agreement between the calculated and the measured air velocities. All average measurements accomplished the validation criterion except from A1 measurements, only for the lowest point.

Figure 11 shows the air velocity profile entering into the building in each vertical axe. A1 air calculations at height lower than 0.9 m are slightly higher than expected. The reason could be the position that is near the vertical window placed in the prevailing wind direction. This is a vertical narrow window from which the complete renewal air enters into the building. Therefore, higher velocities in this non-occupied zone are expected. Consequently, the validation limits are too narrow for the air speed measured at A1 position. Nevertheless, the maximum deviation of measurements rises up to 11.58% at this position, which is an acceptable percentage of deviation taking into account the inlet air velocity variability. Analysing the maximum mean air velocities shown in Table 1, A1

measurements are not acceptable as air speed ranges from 0.3 to 1.71 m/s and the maximum allowed mean air velocity is 0.25 m/s. Nevertheless, higher velocities than 0.4 m/s take place mainly in the non-occupied zone as shown in Figure 12, which shows 0.15 m/s as average air speed in the occupied zone. Figure 12 shows the air velocity modulus distribution in the occupied and non-occupied indoor volume. The CFD cells that accomplish each velocity condition are grouped in Figure 12.

A2 position is placed near the opened window in the secondary room from which indoor air comes out of the building. Although measurements are done in a non-occupied area near the window, air velocity results are near the maximum mean air velocity for indoor environment category C.

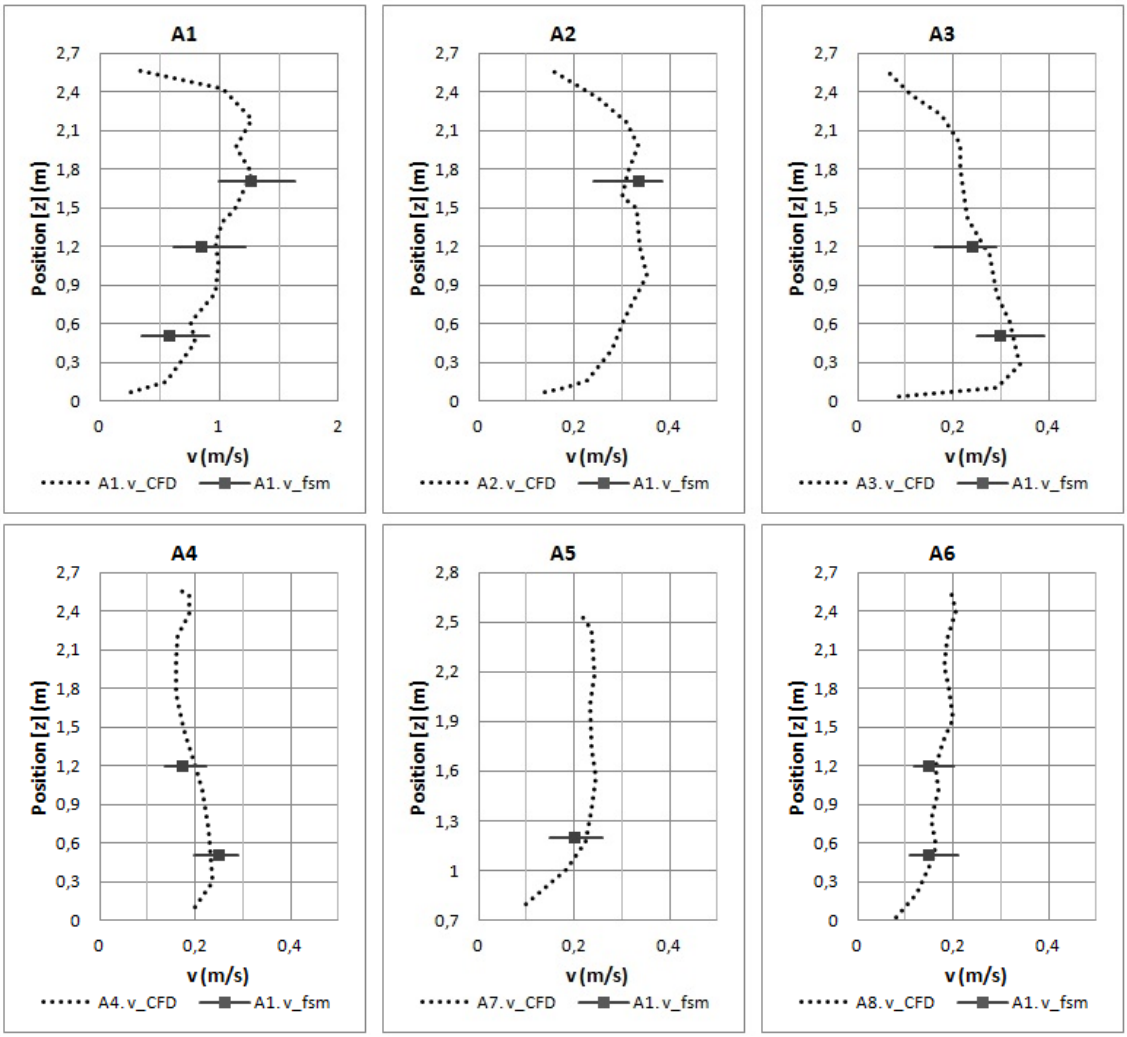

Figure 11. CFD and full-scale measurements comparison. Axes 1 to 6.

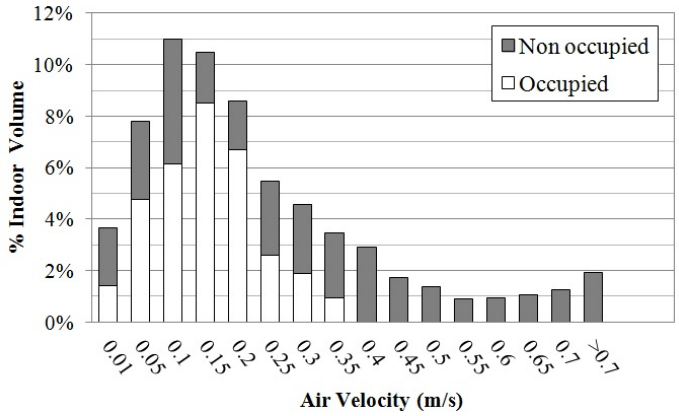

Figure 12. Air velocity distribution in the indoor volume.

The corridor is a delicate area regarding comfort conditions approach. It is placed between the main and the secondary room and it is aligned with the air coming from the main air inlet (ESE vertical window) in the prevailing air direction (ESE). Consequently, air velocities in the corridor are expected to be slightly higher than the maximum allowable value for category C [20]. Figure 11 shows A3 air average velocities ranged between 0.18 and 0.33 m/s. The corridor is a passageway and the air velocity deviation is reasonable in comparison with the inlet air velocities, so it is considered as acceptable.

Additional measurements are done to assess the behaviour of the computational model with the real scenario in the occupied zone (A4, A5 and A6). Figure 11 shows a suitable air prediction. Besides, measurements are lower than the maximum mean air velocity value (category C) [20].

To quantify the difference between the values predicted by the CFD model and the values actually measured (A1 to A6), the root-mean-square error (RMSE) is used. RMSE is defined by the eq (14).

$$RMSE = \sqrt{\sum_{i=1}^{N} \frac{\left(\phi_i - \phi_{i,obs}\right)^2}{N}} \tag{14}$$

where $\emptyset_i$ is the predicted value for i point, $\emptyset_{i,obs}$ is the mean measured value for i point and N is the number of analysed points. The deviation in relative terms is acceptable, with RMSE = 7.49. The discordances between the measurements and the models are lower than 7.5.

In conclusion, the compared data have a physical sense and the air velocities magnitude order between the CFD model and the full-scale measurements are within the validation criterion established [33].

3.2. Indoor comfort conditions analysis

Natural ventilation creates a particular indoor environment. On the one hand, NV is an efficient method to improve the indoor comfort conditions. On the other, NV could lead to high air velocities that may cause discomfort. Moreover it could have significant effects on the indoor temperatures distribution producing temperature fluctuations that may cause undesired comfort conditions. In this particular case, comfort conditions are evaluated through indicators such as *DR*, *PMV* and *PPD*

under steady conditions. The indoor conditions dynamic changes and its fluctuation implications on comfort conditions should be assessed in the future.

Regarding the *PMV*, it depends on occupant and environmental parameters. It considers the occupants' physical activity (metabolic rate of people who work in an office with light activity, M = 93 W/m^2) and the thermal resistance of their clothing (during the summer period the thermal clothing insulation considering no active work, *Icl* is set at 0.5 clo and the corresponding clothing area factor *Fcl* is set at 1.15). The convective heat transfer coefficient is set at hc = 4.6863 W/m^2·K. Air temperature values should be set in the indexes formulas. The limiting temperatures of each indoor environment category described in Table 1 are used to cover a wide range of possible environmental conditions (24.5 ºC, 25.5 ºC and 26 ºC in each simulation). The external wind velocity boundary condition is set at three different values for each air temperature in order to cover a wide velocity range and to determine its impact on indoor comfort conditions: 3.05 m/s, 1.58 m/s and 4.52 m/s.

3.2.1. *DR* analysis

First of all, draught risk is lower for people feeling warmer and higher for people feeling cooler for the whole body [21]. Figure 13 shows the *DR* distribution in the occupied zone (in percentage). *DR* is kept below Category A indoor environment limit (15%, for the tested conditions). *DR* remains concentrated around *DR* = 3% with a temperature increase from 24.5 ºC to 26 ºC for lower air velocities (1.58 m/s). When air velocity is increased, *DR* rate is spread in the indoor environment. *DR*, ranged between 5% and 13%, is distributed in lower volume percentages (between 12% and 16%). Then *DR* comfort index has no critical values to achieve a comfortable indoor environment (*DR* < 15%).

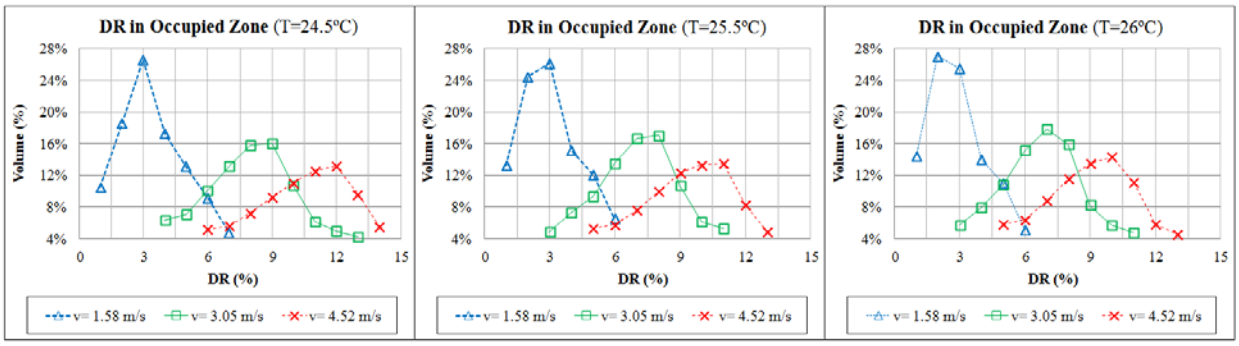

Figure 13. Draught Risk distribution in occupied zone.

The highest tested indoor air temperature does not influence *DR* as shown in figure 13; the three graphs have approximately the same air velocity distribution shape for each temperature. *DR* is almost concentrated at *DR* = 3% for v = 1.58 m/s; *DR* follows a normal distribution with an average value at *DR* = 8% for v = 3 m/s and *DR* = 11% for v = 4.5 m/s.

Nevertheless, the higher *DR* is calculated in the non-occupied zone. Figure 14 shows how the highest *DR* is located in front of the vertical ESE window, near the main room WNW wall and along the passageway. Although higher *DR* is achieved in these places, *DR* is lower than 20% in the whole building. Then, the complete building is classified as Category B attending to *DR* calculation.

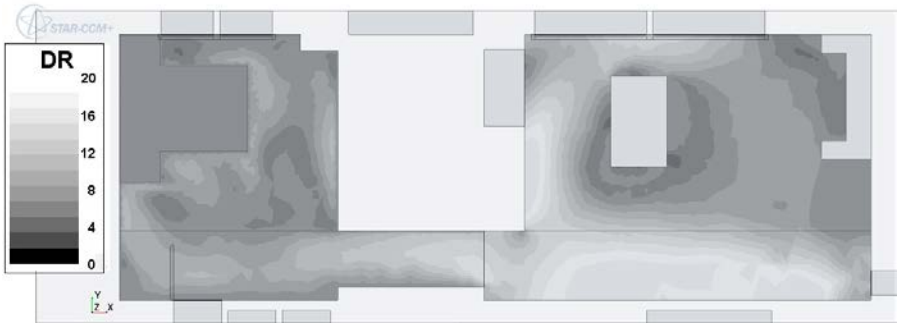

Figure 14. Draught Risk distribution at h = 0.6 m, T = 24.5 ºC.

In conclusion, NV achieves an acceptable *DR* distribution in the occupied zone for the prevailing wind during the warm season.

3.2.2 *PMV* analysis

Although *DR* is lower than 15% in the occupied zone, the building could not be classified as Category A [20] due to the other comfort indexes. Then, figure 15 presents the *PMV* distribution in the occupied zone (occupied volume in %) for each indoor air temperature and wind velocity tested. *PMV* index is kept between 0.2 and 1 (almost neutral, slightly warm) for all tested conditions. Moreover, the air velocity *PMV* effect is almost negligible if wind velocity is lower than 3 m/s. In summer conditions, for people feeling warm in their body, an air movement increase will decrease the warm discomfort and will therefore be beneficial. *PMV* index shows this phenomenon in the building. Although *PMV* is kept in a narrow range for all tested conditions, Figure 15 shows how *PMV* index is slightly improved for higher wind velocities (4.5 m/s). However, *PMV* is not as concentrated as for lower wind velocities (1.58 m/s and 3 m/s), in which 80% of the volume has the same *PMV* index (*PMV* = 0.5 for *T* = 24.5 ºC; *PMV* = 0.75 for *T* = 25.5 ºC and *PMV* = 0.88 for *T* = 26 ºC).

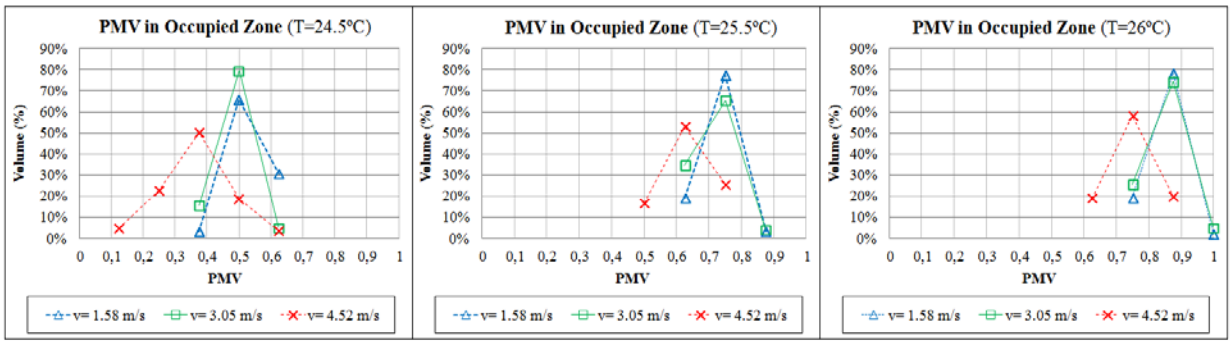

Figure 15. *PMV* index distribution in occupied zone.

According to *PMV* comfort index, the indoor environment cannot be classified as Category A as *PMV* is higher than 0.2 in the occupied zone. The indoor environment is classified as Category B for indoor air temperature lower than 25.5 ºC and higher temperatures means Category C [20].

3.2.3. *PPD* analysis

Figure 16 presents *PPD* distributions in the occupied volume (in %) for each indoor air temperature and each wind velocity. Similar to *PMV*, the indoor environment could neither be classified as Category A according *PPD* comfort index, since it is higher than 6% for almost the whole occupied zone. Nevertheless, it is classified as Category B for T = 24.5 ºC and Category C for higher temperatures. Figure 16 shows that *PPD* ranged between 6% and 17% in most of the occupied zone. Lower wind velocities have *PPD* index more concentrated than high wind velocities. Predicted dissatisfied people are more spread along the occupied volume for air velocities higher than 3 m/s. Figure 16 shows that people feel more comfortable with higher than with lower air velocities in summer conditions, as it is expected.

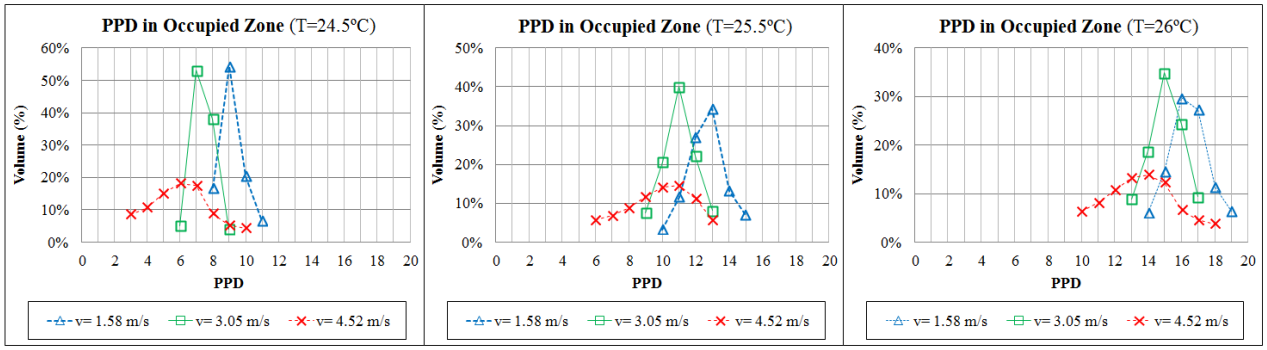

Figure 16. *PPD* index distribution in occupied zone.

PPD in the occupied zone for T = 24.5 ºC and lower air velocities (1.58 m/s) is similar than *PPD* in the occupied zone for T = 25.5 ºC and higher air velocities. *PPD* ranges between 8% and 12% is concentrated in 99% of the occupied zone for case T = 24.5 ºC and v = 1.58 m/s; *PPD* ranges between the same interval are concentrated in 61% of the occupied zone for case T = 25.5 ºC and v = 4.5 m/s. Similarly, *PPD* ranges between 11% and 15% are concentrated in 93% of the occupied zone for case T = 25.5 ºC and v = 1.58 m/s; *PPD* ranges between the same interval are concentrated in 58% of the occupied zone for case T = 26 ºC and v = 4.5 m/s. This calculation demonstrates that *PPD* comfort index belonging to a lower indoor air temperature is ≈ 60% achieved with higher indoor air temperatures and higher air velocities. Therefore, the wind-driven NV effect improves the energy savings by increasing the target indoor temperature, maintaining 60% the predicted percentage of people likely to feel uncomfortable. In other words, comfort feeling associated with a lower indoor air temperature is achieved by increasing air velocity using a non mechanical system such as NV.

4. Conclusions

The paper presents the results of a numerical and experimental research carried out to analyse natural ventilation (NV) effect on indoor comfort conditions and assess the energy efficiency potential improvement. The research is done in case study building that had been previously designed to maximize its NV behaviour since the building design stage. Computational fluid

dynamic (CFD) techniques are used to simulate the NV behaviour through the building and calculate comfort conditions indexes in the indoor environment. The energy efficiency strategy aims to slightly increase the indoor temperature without compromising the initial comfort conditions. The slightly increased temperature feeling should be compensated by increasing the air velocity by means of NV.

Firstly, experimental full-scale measurements are used to validate the CFD model. The CFD calculations show a good agreement with the full-scale measurements. The comparison shows a root-mean-square error lower than 7.5%. Secondly, the simulation is used to calculate and visualize comfort conditions indexes at different conditions in the warm season. Three air temperatures and three wind speeds are carefully chosen to represent a wide range of summer environmental typical conditions, according to recorded temperatures in the measurement conditions. Comfort conditions are assessed through the indexes draught risk (*DR*), predicted mean vote (*PMV*) and predicted percentage of dissatisfied people (*PPD*). The CFD results show no risk of draught in the occupied zone. *DR* is kept under Category A value (*DR* < 15%) [20] for all tested conditions. Nevertheless, local discomfort due to draught is higher in the non-occupied area. Depending on the indoor air temperature and *PMV* and *PPD* indexes, the indoor environment could be classified as Category B or C. In any case the indoor environment is classified as “slightly warm” (*PMV* between 0.5 and 1) and *PPD* is lower than Category C limit, 15%.

The conclusion is that the NV strategy could manage to increase the indoor air temperature 1 ºC maintaining no draught risk and 60% the percentage of people likely to feel uncomfortable. Thus, energy savings are achieved due to the indoor air temperature increase without compromising the initial comfort conditions. Otherwise additional mechanical system should be necessary to maintain the comfort conditions if the indoor air temperature is increased. The energy needs of the building are then reduced. Thereby, a proper NV focus during the initial design stage could improve the building energy efficiency without compromising the indoor comfort conditions.

The ultimate aim of the research is to add a reliable NV behaviour analysis by CFD techniques and achieve more environmentally friendly buildings. Further research should include the analysis of air fluctuation and thermal behaviour (buoyancy effect, thermal inertia, radiation, etc.) implications on comfort conditions. Different opening distributions and winter conditions should be also analysed in the future.

Acknowledgments

The research was done within the frame of "EDIFICACIÓN ECO EFICIENTE, E3” (E3 eco efficient building design) research project at Universitat Politècnica de València.

The meteorological information has been provided by the Spanish State Meteorological Agency, Ministry of Agriculture and Fisheries, Food and Environment. It is forbidden its total or partial reproduction by any other means.

Conflict of interest

The authors declare no conflict of interest.

References

1. Kudryashova A, Genkov A, Mo T (2015) Certification schemes for sustainable buildings: assessment of BREEAM, LEED and LBC from a strategic sustainable development perspective. Blekindge Institute of Technology, Karlskrona.
2. Taleb HM (2015) Natural ventilation as energy efficient solution for achieving low-energy houses in Dubai. *Energy Build* 99: 284-291.
3. U.E. Environmental Protection Agency (EPA), Green building basic information, 2014. Available from: http://www.epa.gov/greenbuilding/pubs/about.htm.
4. Luo ZW, Zhao JN, Gao J, et al. (2007). Estimating natural-ventilation potential considering both thermal comfort and IAQ issues. *Build Environ* 42: 2289-2298.
5. Hitchin ER, Wilson CB (1967) A review of experimental techniques for the investigation of natural ventilation in buildings. *Build Sci* 2: 59-82.
6. Chen Q (2009) Ventilation performance prediction for buildings: A method overview and recent applications. *Build Environ* 44: 848-858.
7. Coakley D, Raftery P, Keane M (2014) A review of methods to match building energy simulation models to measured data. *Renew Sustain Energy Rev* 37: 123-141.
8. Zhu YX, Luo MH, Ouyang Q, et al. (2015) Dynamic characteristics and comfort assessment of airflows in indoor environments: A review. *Build Environ* 91: 5-14.
9. Etheridge D (2015) A perspective on fifty years of natural ventilation research. *Build Environ* 91: 51-60.
10. Wang H, Lin H, Ng VCY, et al. (2015) Failure of natural ventilation strategy in a sustainable house in China. *Int J Low-Carbon Tech* 10: 216-228.
11. Moosavi L, Mahyuddin N, Abghafar N, et al. (2014) Thermal performance of atria: an overview of natural ventilation effective designs. *Renew Sustain Energy Rev* 34: 654-670.
12. Foucquier A, Robert S, Suard F, et al. (2013) State of the art in building modelling and energy performances prediction: A review. *Renew Sustain Energy Rev* 23: 271-288.
13. Mora-Pérez M, Guillén-Guillamón I, López-Jiménez PA (2015) Computational analysis of wind interactions for comparing different buildings sites in terms of natural ventilation. *Adv Eng Softw* 88: 73-82.
14. Sun YM, Zhang WY, Zhang CY (2014) Preliminary study on natural ventilation for hospital building in hot and humid regions. 30th International Plea Conference. CEPT University, Ahmedabad.
15. Zhou CB, Wang ZQ, Chen QY, et al. (2014) Design optimization and field demonstration of natural ventilation for high-rise residential buildings. *Energy Build* 82: 457-465.
16. Van Hooff T, Blocken B, Aanen L, et al. (2011) A venturi-shaped roof for wind-induced natural ventilation of buildings: wind tunnel and CFD evaluation of different design configurations. *Build Environ* 46: 1797-1807.
17. Liu PC, Lin HT, Chou JH (2009) Evaluation of buoyancy-driven ventilation in atrium buildings using computational fluid dynamics and reduced-scale air model. *Build Environ* 44: 1970-1979.
18. Hughes BR, Calautit JK, Ghani SA (2012) The development of commercial wind towers for natural ventilation: A review. *Appl Energy* 92: 606-627.

19. Mora-Pérez M, Guillén-Guillamón I, López-Patiño G, et al. (2016) Natural ventilation building design approach in Mediterranean regions—A case study at the Valencian coastal regional scale (Spain). *Sustain* 8: 855.
20. ISO Standard 7730 (2005) Ergonomics of the thermal environment—Analytical determination and interpretation of thermal comfort using calculation of the PMV and PPD indices and local thermal comfort criteria.
21. AENOR (2008) AEN/CTN 100. UNE-CR 1752:2008. Ventilation for buildings—Design criteria for the indoor environment. Comité técnico, Spain. Available from: http://www.aenor.es.
22. ANSI/ASHRAE (2013) Thermal environmental conditions for human occupancy.
23. Gagliano A, Nocera F, Patania F, et al. (2016) Synergic effects of termal mass and natural ventilation on the termal behaviour of traditional massive buildings. *Int J Sustain Energy* 35: 411-428.
24. CD-Adapco. Star CCM+ User's Manual. Available from: www.cd-adapco.com.
25. Franke J, Hellsten A, Schlünzen H, et al. (2007) Best practice guideline for the CFD simulation of flows in the urban environment. *Cost Off Bruss* 44:1-52.
26. Wieringa J (1992) Updating the Davenport roughness classification. *J Wind Eng Ind Aerodyn* 41: 357-368.
27. Agencia Estatal de Meteorología de España (AEMET). Spanish State Meteorological Agency, Ministry of Agriculture and Fisheries, Food and Environment. Available from: http://www.aemet.es.
28. Windfinder. Available from: http://es.windfinder.com/windstats/windstatistic_valencia.htm.
29. Manwell, JF, Mcgowan, JG, Rogers, AL (2009) *Wind energy explained: theory, design and application*, 2 Eds., Wiley.
30. Peterson EW, Hennessey JP (1977) On the use of power laws for estimates of wind power potential. *J Appl Meteorol* 17.
31. Justus CG, Mikhail A (1976) Height variation of wind speed and wind distributions statistics. *Geophys Res Lett* 3: 261-264.
32. Ray SD, Gong NW, Glicksman LR, et al. (2014) Experimental characterization of full-scale naturally ventilated atrium and validation of CFD simulations. *Energy Build* 69: 285-291.
33. Shao JT, Liu J, Zhao JN (2012) Evaluation of various non-linear k-epsilon models for predicting wind flow around an isolated high-rise building within the surface boundary layer. *Build Environ* 57: 145-155.
34. García JAO, (2010) A review of general and local thermal comfort models for controlling indoor ambiences, In: Kumar, A. Author, *Air Quality*, InTech, 309-326.
35. Fanger, PO (1972) *Thermal comfort—Analysis and applications in environmental engineering*, Kingsport Press.
36. Reglamento de Instalaciones Térmicas en los Edificios (RITE). Ministerio de Industria, Energía y Turismo, Gobierno de España. Available from: http://www.minetur.gob.es/energia/desarrollo/EficienciaEnergetica/RITE/Paginas/InstalacionesTermicas.aspx.
37. EN 13779:2007. Ventilation for non-residential buildings—Performance requirements for ventilation and room-conditioning systems. April 2007.
38. Hajdukievwicz M, Geron M, Keane MM (2013) Formal calibration methodology for CFD models of naturally ventilated indoor environments. *Build Environ* 59: 290-302.

39. Van Hooff T, Blocken B (2010) On the effect of wind direction and urban surroundings on natural ventilation of a large semi-enclosed stadium. *Comput Fluids* 39: 1146-1155.
40. Lo LJ, Novoselac A (2012) Cross ventilation with small openings: Measurements in a multi-zone test building. *Build Environ* 57: 377-386.
41. Franke J, Hirsch C, Jensen AG, et al. (2004) Recommendations on the use of CFD in wind engineering. In: van Beeck, J.P.A.J. (Ed.), *Proceedings of the International Conference Urban Wind Engineering and Building Aerodynamics*, von Karman Institute.

AIMS Press